Physicochemical Behavior of Ce-doped UO_2

Jeongmook Lee[a]*, Dong Woo Lee[a], Hwakyeung Jeong[a], Jong-Yun Kim[a,b] and Sang Ho Lim[a,b]
[a]Nuclear Chemistry Research Team, Korea Atomic Energy Research Institute, 111 Daedeok-daero 989 Beon-gil, Yuseong-gu, Daejeon, 34057, Republic of Korea
[b]Department of Radiochemistry & Nuclear Nonproliferation, University of Science & Technology, Gajeong-ro 217, Yuseong-gu, Daejeon, 34113, Republic of Korea
*Corresponding author: leejm@kaeri.re.kr

1. Introduction

Lattice-doped UO_2 pellets have been used as the simulated fuels to investigate the physical and chemical properties of spent nuclear fuel [1-5]. Because of spent nuclear fuel is consisted of mainly UO_2 (95%) and minor elements such as radioactive fission products and actinides, lattice-doped UO_2 is good model system to confirm influence of those minor elements on physicochemical behavior of UO_2. For example, Gd-doped UO_2 was prepared and investigated to study the influences of trivalent rare earth on structure and corrosion of UO_2 [3,4]. Its physical and chemical properties could be useful information to make strategies for long-term management of spent nuclear fuel including deep geological disposal.

In this study, Ce-doped UO_2 have been investigated the effect of Ce-doping on the UO_2 structure and its electrochemical behavior.

2. Experimental

Ce-doped UO_2 sample pallets with various doping level were prepared by powder blending method. UO_2 and CeO_2 powders with appropriate compositions were finely blended and mixed. The powder mixtures were pelletized and sintered at 1700℃ for 18 h in hydrogen atmosphere. After then, those were annealed in same atmosphere at 1200℃ for 12 h.

The surface structure of the sample pellets was analyzed and characterized using scanning electron microscopy (SEM), X-ray diffraction (XRD) and Raman spectroscopy. The morphologies of sample surface were obtained by SEM using 20 keV electron acceleration voltage at 10 mm working distance. XRD data was collected by Bruker D8 Advance using CuKα line source (beam current 40mA at 40kV). The lattice parameters of the samples were calculated from XRD spectra with the refinement process. Raman spectra were acquired using ANDOR Shamrock SR500i spectrometer with a 633 nm excitation wavelength He-Ne laser

Ce-doped UO_2 electrode was prepared as mounting pellets onto steel-working electrode to study its electrochemical behavior. Three electrode system is used for cyclic voltammetry (CHI-600D, USA) and RDE system of 1000 rpm (PINE, USA) in carbonate/bicarbonate dissolved in 0.1 M NaCl solution ($[HCO_3^-/CO_3^{2-}]$=0.01 mol L^{-1}).

3. Results

The grain size observed in SEM images of Ce-doped UO_2 decreased with increasing doping level. The lattice parameters of Ce-doped UO_2 linearly decreased with increasing Ce doping level. This linear relationship was also observed for Gd- and Nd-doped UO_2 [3,5], and represented that sample pellets were formed as a solid solution. Those changes of the grain size and lattice parameter should be strongly related to the substituted cation because trivalent cation (Ce^{3+}) induce the creation of oxygen vacancy which has smaller apparent radius than that of oxygen, although Ce has another stable cation, Ce^{4+}.

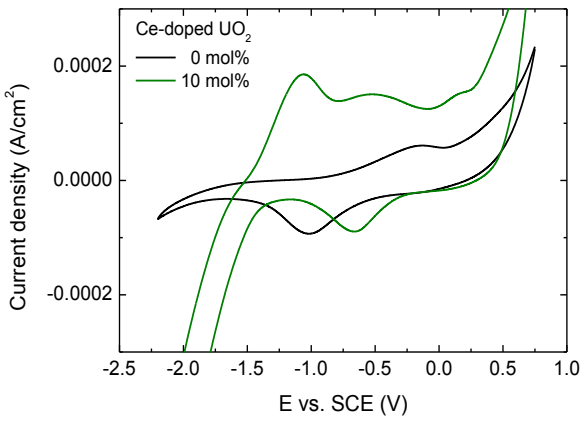

Fig. 1. Cyclic voltammogram of Ce doped UO_2 in 0.1 M NaCl containing $[HCO_3^-/CO_3^{2-}]$=0.01 mol L^{-1} solution (pH=10). Scan rate is 0.01 V sec^{-1}.

Raman spectrum of Ce-doped UO_2 sample pallet showed two distinct peaks. The peak shown at ~445 cm^{-1} has been assigned to U-O symmetric stretching mode in the fluorite structure [6-8]. Small and broad peak at ~ 1150 cm^{-1} is ascribed to an overtone of the first order longitudinal optical phonon mode regarded as fingerprint for quasi-perfect fluorite structure [9,10]. There was the broad feature at 500 ~ 650 cm^{-1}. This is mainly formed by the peak at ~ 530 cm^{-1} representing defect due to oxygen vacancy associated with trivalent cation. This result strongly supports that Ce in our sample should exist as Ce^{3+} form. The intensity of this peak increased with increasing Ce doping level, as

shown in similar cases like Gd- and La-doped UO_2. Gd-, Nd-, and La-doped UO_2 have similar intensity of peak at ~ 530 cm^{-1} for same doing level. However, Ce-doped UO_2 shows higher peak intensity at same position although it has same doping level with Gd- and Nd-doped UO_2. It is expected that Ce doping has a significant influence on defect structure formation by oxygen vacancy.

Fig. 1 shows cyclic voltammograms recorded in carbonate solutions. The anodic oxidation current at about –0.2 V indicates forming the oxidation of a thin surface layer mixed with U(IV) and U(V). It moves from –0.2 V to 0.1 V as increasing Ce doping level. This can be explained with that the doped Ce inhibit oxidation of UO_2 matrix surface and delay the followed dissolution of UO_2 electrode ranged over 0.2 V. This electrochemical behavior could be related the oxygen vacancy induced by Ce^{3+} doping. To define this influence, more microscopic analysis technique and detail interpretation would be applied.

4. Conclusions

The structure of Ce-doped UO_2 with various doping levels was characterized by SEM, XRD and Raman spectroscopy. The electrochemical behavior of sample was also investigated by cyclic voltammetry method. Ce doping formed the oxygen vacancy and the smaller grain size in UO_2 surface structure like other trivalent doping elements, Gd^{3+}, Nd^{3+} and La^{3+}. It means that Ce in our sample also exists as Ce^{3+}. However, Ce doping more affected the creation of defect due to oxygen vacancy associated with trivalent cation than Gd, Nd and La doping. It was also shown that Ce doping inhibits the surface oxidation of UO_2 matrix.

ACKNOWLEDGEMENT

This work was supported by the National Research Foundation of Korea (NRF) grant funded by the Korean government (MSIT) (2017M2A8A5014754)

REFERENCES

[`] L. Desgranges, Y. Pontillon, P. Matheron, M. Marcet, P. Simon, G. Guimbretie, et al., Miscibility Gap in the U−Nd−O Phase Diagram : a New Approach of Nuclear Oxides in the Environment?, Inorganic Chemistry, Vol.51, pp. 9147–9149, 2012.

[2] Z. Talip, T. Wiss, P.E. Raison, J. Paillier, D. Manara, J. Somers, et al., Raman and X-ray Studies of UraniumLanthanum-Mixed Oxides Before and After Air Oxidation, Journal of American Ceramic Society, Vol.98, pp. 2278–2285, 2015.

[3] J. Lee, J. Kim, Y.-S. Youn, N. Liu, J.-G. Kim, Y.-K. Ha, D. W. Shoemith, and J.-Y. Kim, Raman study on structure of U1-yGdyO2-x (y=0.005, 0.01, 0.03, 0.05 and 0.1) solid solutions, Journal of Nuclear Materials, Vol.486, pp. 216-221, 2017.

[4] J. Kim, J. Lee, Y.-S. Youn, N. Liu, J.-G. Kim, Y.-K. Ha, S.-E. Bae, D. W. Shoemith, and J.-Y. Kim, The Combined Influence of Gadolinium Doping and Non-stoichiometry on the Structural and Electrochemical Properties of Uranium Dioxide, Electrochimica Acta, Vol.247, pp. 942-948, 2017.

[5] J. Lee, J. Kim, Y.-S. Youn, J.-Y. Kim and S. H. Lim, Surface characterization of (U,Nd)O2: the influence of trivalent-dopant on structure of UO2, Progress in Nuclear Science and Technology Vol.5, pp. 33-36, 2018.

[6] G.C. Allen, I.S. Butler, Characterisation of uranium oxides by micro-Raman spectroscopy, Journal of Nuclear Materials, Vol.144, pp. 17–19, 1987.

[7] P.R. Graves, Raman Microprobe Spectroscopy of Uranium Dioxide Single Crystals and Ion Implanted Polycrystals, Applied Spectroscopy, Vol.44, pp. 1665–1667, 1990.

[8] G.M. Begun, R.G. Haire, W.R. Wilmarth, J.R. Peterson, Raman spectra of some actinide dioxides and of EuF2, Journal of the Less Common Metals, Vol.162, pp. 129–133, 1990.

[9] D. Manara, B. Renker, Raman spectra of stoichiometric and hyperstoichiometric uranium dioxide, Journal of Nuclear Materials, Vol. 321, pp. 233–237, 2003.

[10] T. Livneh, E. Sterer, Effect of pressure on the resonant multiphonon Raman scattering in UO2, Physical Review B, Vol.73, p. 085118, 2006.